Journal of Power Sources 196 (2011) 8444–8449

Contents lists available at ScienceDirect

Journal of Power Sources

journal homepage: www.elsevier.com/locate/jpowsour

# Multi-loop control strategy of a solid oxide fuel cell and micro gas turbine hybrid system

Xiao-Juan Wu[a,*], Xin-Jian Zhu[b]

[a] School of Automation, University of Electronic Science and Technology of China, Chengdu 610054, China
[b] Institute of Fuel Cell, Shanghai Jiao Tong University, Shanghai 200030, China

ARTICLE INFO

*Article history:*
Received 23 March 2011
Received in revised form 25 May 2011
Accepted 26 May 2011
Available online 2 June 2011

*Keywords:*
Solid oxide fuel cell
Micro gas turbine
Multi-loop control

ABSTRACT

Solid oxide fuel cell and micro gas turbine (SOFC/MGT) hybrid system is a promising distributed power technology. In order to ensure the system safe operation as well as long lifetime of the fuel cell, an effective control manner is expected to regulate the temperature and fuel utilization at the desired level, and track the desired power output. Thus, a multi-loop control strategy for the hybrid system is investigated in this paper. A mathematical model for the SOFC/MGT hybrid system is built firstly. Based on the mathematical model, control cycles are introduced and their design is discussed. Part load operation condition is employed to investigate the control strategies for the system. The dynamic modeling and control implementation are realized in the MATLAB/SIMULINK environment, and the simulation results show that it is feasible to build the multi-loop control methods for the SOFC/MGT hybrid system with regard to load disturbances.



## 1. Introduction

Among the fuel cell, solid oxide fuel cell (SOFC) is a high temperature fuel cell (600–1000 °C), which allows not only high fuel cell efficiency but also the additional possibility of its acting as a high temperature heat source for various gases [1]. The most beneficial way of utilizing this potential is to smoothly combine with the micro gas turbine (MGT).

It is important to ensure system stability and performance for maximum service life. Thus, one important challenge for the SOFC/MGT hybrid system is to design control strategies for the system operating under different working conditions, especially for the part-load operation. Under various loads, SOFC operating temperature and turbine inlet temperature have great influences on the performance of the SOFC/MGT hybrid system [2]. Consequently it is necessary to find a suitable control method to control the temperature in a specified range with smaller fluctuation. For the SOFC/MGT hybrid system, too low fuel utilization leads to low steam content in the anode recycle and the high turbine inlet temperature and therewith the risk of carbon deposition and compressor surge. On the other hand, too high fuel utilization leads to steep internal temperature gradients in the fuel cell and herewith advances thermal cracking. Thus, the fuel utilization is usually kept within the range from 75% to 90%. In addition, load transient often involves significant peaks in power relative to the steady-state load, so the power plant should be controlled to deliver the desired power output.

During the last several decades, many researchers have made great efforts on SOFC/MGT hybrid system modeling to improve its performance. However, few studied the part-load operation and control strategies. A detailed dynamic model was presented and feedback control strategy was proposed to control the SOFC temperature and output power of a SOFC/MGT hybrid system in Ref. [3]. The power and SOFC operating temperature control in a biomass gas fueled SOFC/MGT hybrid system were discussed in Ref. [4]. In Ref. [5], an integrated model for a load-connected SOFC/GT hybrid system was introduced firstly, and then PI controllers were employed to control the SOFC operating temperature and fuel utilization. In Ref. [6], a feedback control was used to control the SOFC operating temperature and combustor temperature during the transient. All the simulation results gave satisfactory results. However, the SOFC/MGT hybrid system is a multivariable and strong coupling nonlinear system, how to decouple the coupling thermal system and design practical controllers are not considered in the open literatures. Moreover, most of the controllers have not considered the thermal, power and fuel utilization control at the same time.

Therefore, the project of this article is to present a comprehensive control layout for the SOFC/MGT hybrid system. The system has four control variables, which are power, SOFC operating temperature, turbine inlet temperature and fuel utilization. The manipulated variables are current, fuel flow, air flow, etc. There

* Corresponding author. Tel.: +86 21 34203657; fax: +86 21 62932154.
*E-mail address:* xj2_wu@hotmail.com (X.-J. Wu).

0378-7753/$ – see front matter 
doi:10.1016/j.jpowsour.2011.05.075

**Nomenclature**

| | |
|---|---|
| $x_{6,CH_4}$ | inlet methane molar fraction |
| $x_{6,CO}$ | inlet carbon monoxide molar fraction |
| $x_{6,H_2}$ | inlet hydrogen molar fraction |
| $T_{st}$ | SOFC stack temperature (K) |
| $T_{st}^*$ | ideal SOFC stack temperature (K) |
| $T_{TIT}$ | turbine inlet temperature (K) |
| $T_{TIT}^*$ | ideal turbine inlet temperature (K) |
| $u_f$ | fuel utilization |
| $u_f^*$ | ideal fuel utilization |
| $n_1$ | air flow rate (mol $s^{-1}$) |
| $n_6$ | fuel flow rate (mol $s^{-1}$) |
| $n$ | rotate speed (rpm) |
| $r_3$ | hydrogen reaction rate (mol $s^{-1}$) |
| $f_c$ | bypass valve opening |
| $P_{ac}$ | stack power output (kW) |
| $P_{ac}^*$ | desired output power (kW) |
| $e$ | error |
| $i$ | SOFC stack current (A) |

is strong interaction among the manipulated and controlled variables. However, as the required time scales are very different for different control issues, a multi-loop control design may be applied without resulting in instabilities.

In order to design a control system, a nonlinear model that the controller will use is the first step. This model should be as accurate as possible, while being simple enough to allow for calculations. If the mathematical model of the SOFC/MGT hybrid system is applied, it will consume much time to obtain the solutions. For this reason, a nonlinear model of the SOFC/MGT hybrid system is built by a dynamic RBF neural network model. Based on the dynamic RBF identification model, an adaptive Proportional-Integral-Derivative (PID) decoupling control scheme is proposed to control the temperature of the SOFC/MGT hybrid system in a specified range, and a Model Predictive Control (MPC) scheme is built to control the power output within a safety range. In addition, a single neuron adaptive PID controller is applied to reset the fuel utilization to its static value of 85%.

## 2. SOFC/MGT hybrid system model

A topping cycle pressurized SOFC/MGT hybrid system is shown in Fig. 1, which is designed on the basis of the tubular technology pioneered by Siemens Westinghouse in the 1970s [7]. It consists of an anode recirculation SOFC and a micro gas turbine. The pressurized fuel is brought to the mixer to blend with the anode recirculation stream to support the steam reforming reaction in the pre-reformer and anode compartment of the fuel cell. The whole model is implemented in the equation based on modeling tool MATLAB/SIMULINK. The sub-models comprise the following:

- The anode recirculation SOFC model developed in this study is based on the design of Siemens Westinghous. The SOFC stack model consists of electrochemical and thermal models. Details of the SOFC modeling can be found in our previous studies [8]. Assuming that temperature is uniform in a stack, the energy balance equation for the SOFC is [10]:

$$T_{st} = f_1(i, n_1, n_6) \tag{1}$$

The output power of the SOFC stack $P_{ac}$ can be expressed as follows [8]:

$$P_{ac} = f_2(i, n_1, n_6) \tag{2}$$

The fuel utilization of the anode recirculation SOFC system is described by:

$$u_f = \frac{r_3}{n_6 \cdot (4x_{6,CH_4} + x_{6,CO} + x_{6,H_2})} \tag{3}$$

- The catalytic burner is modeled on the basis of the fuel oxidation reactions, assumed to be driven to completion. A single-pass counter-flow plate-fin heat exchanger is chosen here [9]. The temperature of the turbine inlet gas can be determined from [10]:

$$T_{TIT} = f_3(i, n_1, n_6) \tag{4}$$

- Typical compressor and turbine maps are used in the modeling. The ideal temperature of the working fluid at the outlet of the turbine can be obtained from Ref. [10].
- The shaft model includes acceleration/deceleration of the shaft through moment of inertia of the moving parts.

The mathematical model replaces the real SOFC/MGT hybrid system to generate the simulation data required for the identification of the dynamic RBF neural network. The SOFC/MGT hybrid system model developed in MATLAB and the setting parameters can refer to the literature [8].

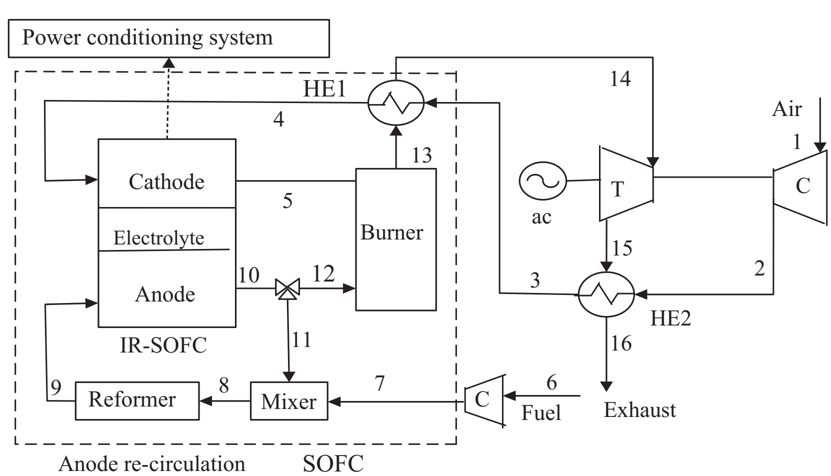


**Fig. 1.** Structure diagram of SOFC/MGT hybrid power system.

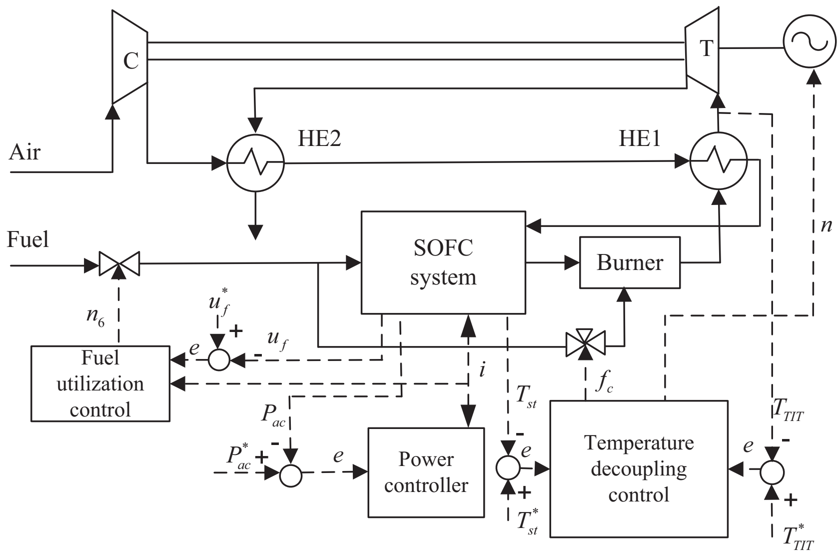


**Fig. 2.** Control structure of SOFC/MGT hybrid system.

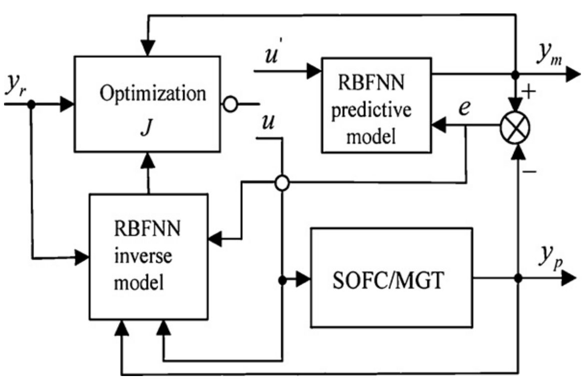


**Fig. 3.** Power tracking control system.

## 3. Control of SOFC/MGT hybrid system

### 3.1. Control scheme design

The main objective is to maintain SOFC temperature and turbine inlet temperature within a small range, to regulate the output power to track the load, and keep the fuel utilization a stable value under the part-load working condition. This goal can be realized by adjusting the control variables such as air flow rate, fuel flow rate, bypass valve opening and current. Due to the strongly different controller time scales, the interaction between various control loops does not lead to instability. Therefore, a multi-loop control design may be applied.

- *Thermal control*: There is strong interaction among the manipulated variables (fuel flowrate and air flowrate) and controlled variables (SOFC operating temperature and turbine inlet temperature), so the coupling thermal system should be decoupled. The inlet air flow can be adjusted by the gas turbine rotate speed $n$, and the fuel flow which enters the burner is controlled by the opening $f_c$ of the bypass valve 2 (BV2) which connects the inlet fuel to the burner. Bypass valve opening is commonly expressed as a percentage that zero means shut-down and one means fully open. So the manipulated variables can be defined as bypass valve opening $f_c$ and rotate speed $n$ (very slow).
- *Power control*: Due to its quick dynamics, power is controlled by manipulating SOFC current. As it is only limited by the electrochemical reaction restoring the charge which has been drained by the load, the fuel cell can respond very quickly to load changes. Typically, time constants of below 1 s are deemed as a change in current [3]. For the primary control of power, it is therefore reasonable to manipulate the current (magnitude of less than one second).
- *Fuel utilization control*: By manipulating the fuel flowrate (magnitude of few seconds).

The mentioned control loops are explained in detail in the following sections. The resulting control system is sketched in Fig. 2. It must be pointed out that the control strategy presented here is adapted to the behavior of the described system. Even though the shown parameters are only valid for this system, it is expected that the control strategy can be adapted to a real system once data of its true behavior are available.

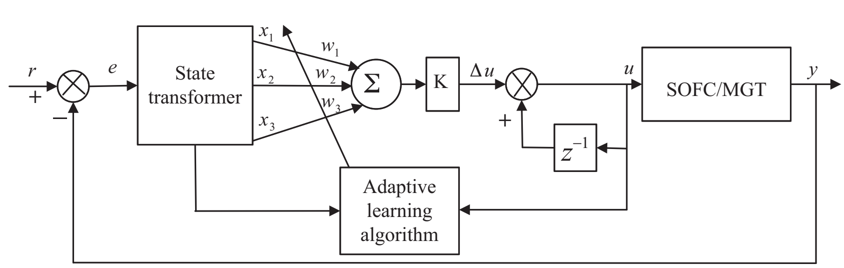


**Fig. 4.** Fuel utilization control structure based on improved single-neural unit adaptive PID control.

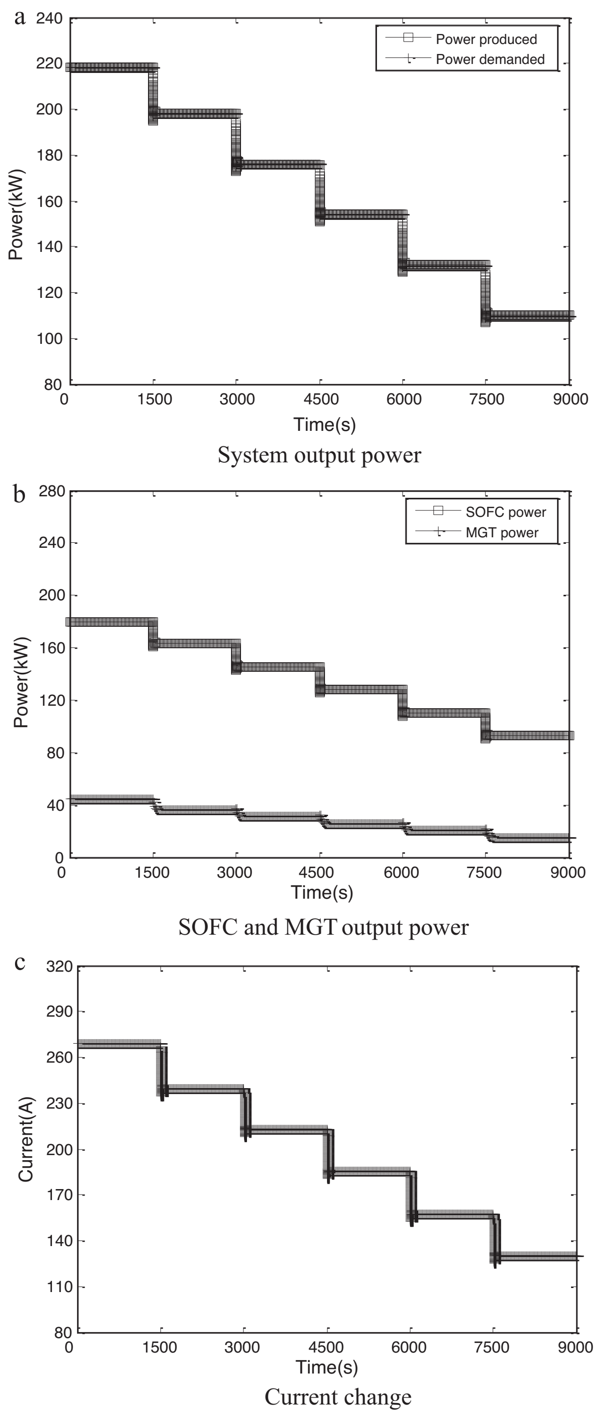


**Fig. 5.** Power dynamic response. (a) System output power. (b) SOFC and MGT output power. (c) Current change.

### 3.2. Thermal decoupling control

The structure for the temperature decoupling control of the SOFC/MGT hybrid system combines the dynamic RBF neural network and the conventional PID controller [11]. The dynamic RBF neural network is used to tune parameters of the conventional PID controller to keep system stable. For two inputs and two outputs system, the coupling effect from the second loop is treated as exterior disturbance to the first main loop. At the same time, the coupling effect from the first loop is treated as exterior disturbance to the second main loop. Then, the PID controller based on the dynamic RBF neural network is used to eliminate the disturbance and improve the tracking performance.

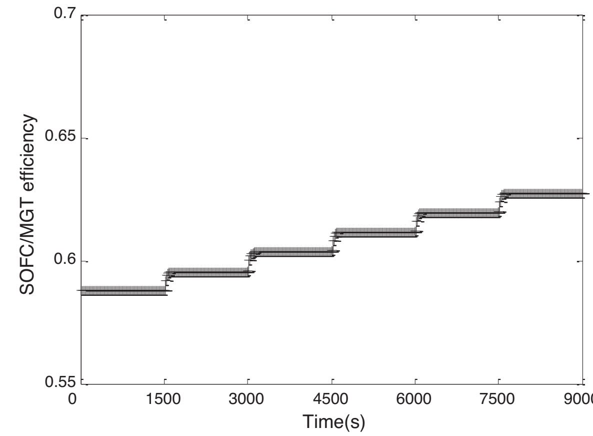


**Fig. 6.** Generating efficiency response.

### 3.3. Power tracking control

The basic frame of the proposed model predictive controller based on the dynamic RBF identification model is shown in Fig. 3. Where, $y_p$ is the real output of the SOFC/MGT hybrid system, $y_m$ the

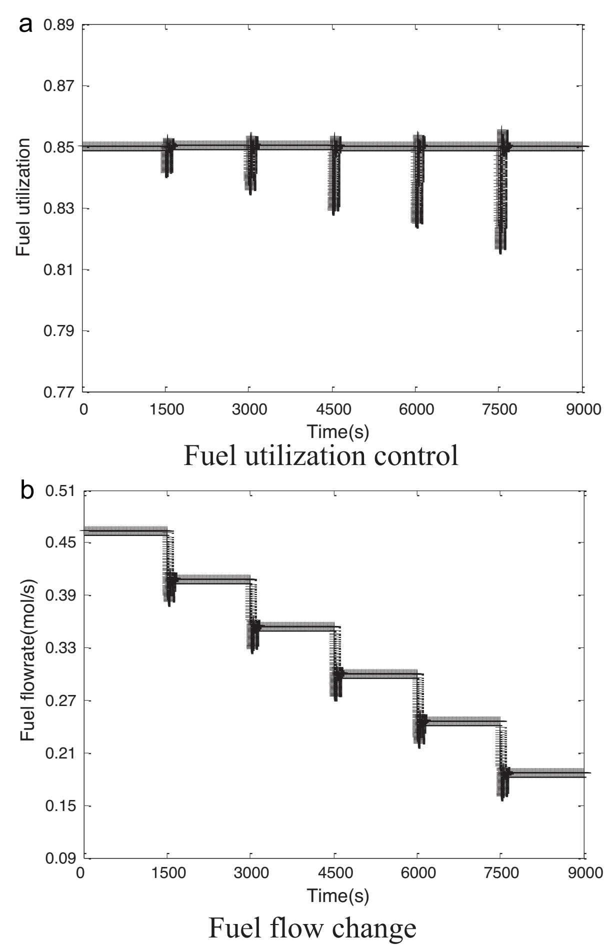


**Fig. 7.** Fuel utilization dynamic response. (a) Fuel utilization control. (b) Fuel flow change.

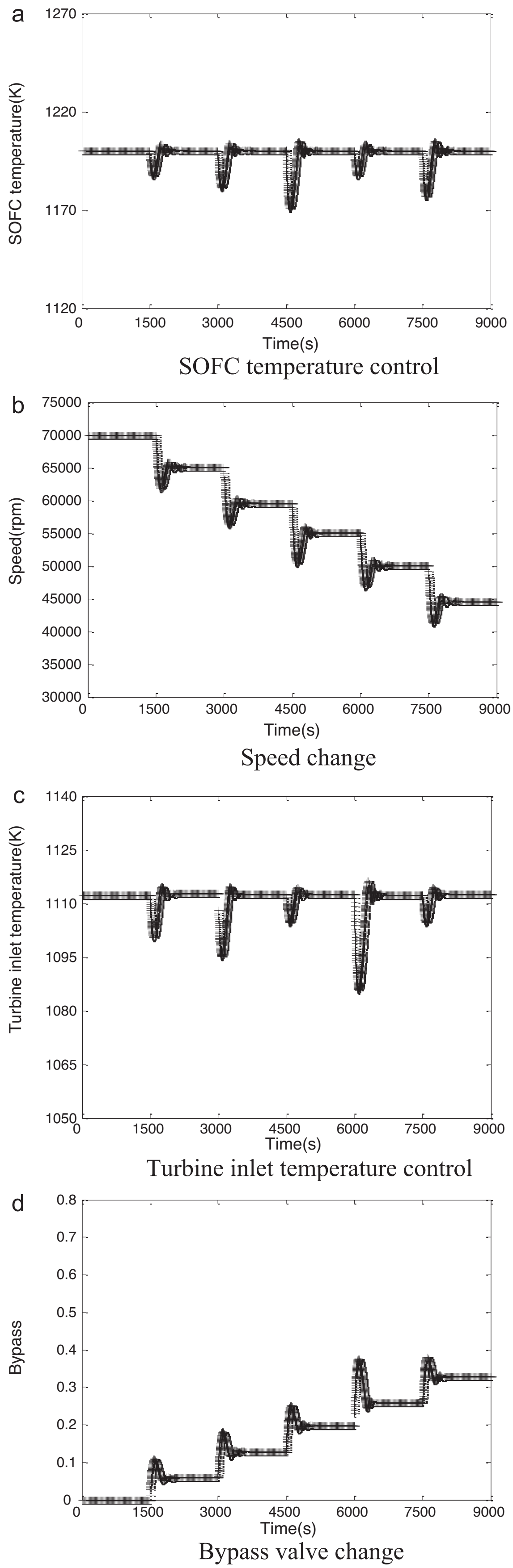


**Fig. 8.** Temperature dynamic response. (a) SOFC temperature control. (b) Speed change. (c) Turbine inlet temperature control. (d) Bypass valve change.

predictive output of the dynamic RBF neural network model. $y_r$ is the reference power defined as follows:

$$y_r(k+1) = c \cdot y(k) + (1-c) \cdot r(k) \tag{5}$$

where $c$ is the gentle factor, $0 \le c \le 1$, and $r(k)$ is the system set value.

The predictive output of feedback system is:

$$y_p(k+j) = e(k) + y_m(k+j) \quad (j = 1, 2, \ldots, P) \tag{6}$$

where $P$ is the predictive horizon, and the error at instance $k$ is defined as:

$$e(k) = y_p(k) - y_m(k) \tag{7}$$

Define the objective function as:

$$J = \min \left\{ \sum_{j=1}^{P} [y_r(k+j) - y_p(k+j)]^2 + \lambda \sum_{j=1}^{M} \Delta u^2(k+j) \right\} \tag{8}$$

$$\Delta u(k+j) = u(k+j) - u(k+j-1) \quad (j = 0, 1, \ldots, (n_u - 1)) \tag{9}$$

$$s.t. \begin{cases} |\Delta u(k+j)| \le \Delta u^{\max} \\ u^{\min} \le u(k+j) \le u^{\max} \\ y^{\min} \le y_p(k+j) \le y^{\max} \end{cases}$$

where $\Delta u(k+j)$ is the increment of controlled signal, $M$ the control horizon, $\lambda$ the weight coefficient. Based on the dynamic RBF neural network model, the object function $J$ is optimized and the optimal output can be obtained. The optimization process can be obtained from Ref. [12].

### 3.4. Fuel utilization control

After a load change, the fuel utilization must be reset to its static value of 85%. This is achieved simply by a single neuron adaptive PID controller, which is shown in Fig. 4. Where $r$ is reference input, $e$ the error, $y$ the feedback, $x_i$ the neuron input, $\omega_i$ corresponding weight, and $K$ is proportion coefficient. The input of neuron is expressed as follows:

$$x_1(k) = e(k) - e(k-1) \tag{10}$$

$$x_2(k) = e(k) \tag{11}$$

$$x_3(k) = e(k) - 2e(k-1) + e(k-2) \tag{12}$$

The output of neuron is described by:

$$\Delta u(k) = K \sum_{i=1}^{3} w_i(k) x_i(k) \quad (i = 1, 2, 3) \tag{13}$$

Single neuron adaptive controller realizes the functions of self-adapting and self-learning by adjusting the weights. Thus, the algorithm to adjust weights is the core of single neuron controller. Based on the quadratic performance index, the weighting coefficient is adjusted with the minimum weighted square sum of the output error and control increment [13].

## 4. Simulation

In this research, part-load operation condition is employed to investigate the control strategies of the SOFC/MGT hybrid system. Firstly, with the physical model, the training data for the dynamic RBF neural network is generated. The width and center of the RBF hidden $b_i$, $c_i$ are chosen on the interval [0, 5] and [−4, 4] respectively, and the connection weight of $i$th hidden node to the $N$th output node $w_{iN}$ is [0, 1]. $b_i$, $c_i$ and $w_{iN}$ are trained on-line. Based on the dynamic RBF neural network, the various control loops are performed.

When the external load of the SOFC/MGT hybrid system has a series of step changes shown in Fig. 5(a), the model predictive controller is used to control the SOFC power. Let the predictive horizon $P = 8$, the control horizon $M = 1$, the gentle factor $c = 0.55$, the weight coefficient $\lambda = 0.45$, the setting value $\varepsilon = 0.05$, the correction factor $\alpha = 1.6$, and searching precision $b_0 - a_0 = 0.08$. The power output of the SOFC/MGT hybrid system tracks the reference power satisfactorily, which is shown in Fig. 5(a). The maximum error of the output power is 3.64%, and the mean steady-state error is 0.11%. The response of the SOFC power output and the MGT power output are respectively shown in Fig. 5(b). From the simulation results, the SOFC output power is the core output power of the SOFC/MGT hybrid system, and the MGT output power changes with the SOFC output power. It is obvious that the response time of the gas turbine is slower than the SOFC after the load change. The reasons are mainly in the following: (1) due to the delay in the mechanical structure and thermal response, the air flow rate control is slow; (2) the fast readjustment of the electrochemical reaction and the fast adjustment of the fuel control valve opening to change the fuel flow rate. Moreover, the ratio of SOFC and MGT power is around 4 according to the output power. The change of the SOFC current is shown in Fig. 5(c). The generating efficiency change of the SOFC/MGT hybrid system is shown in Fig. 6. The simulation results show that it is feasible to adjust the SOFC output power in various loads, which not only tracks the load but improves the generating efficiency.

For the fuel utilization, the setting parameters of the single neuron adaptive PID controller are as follows: proportion coefficient $K = 0.03$, weighting coefficients of the output error and control increment respectively $P = 2.3$, $Q = 1.4$. The proportion, integral and differential learning rate $\partial_P = 60$, $\partial_I = 1.8$, $\partial_D = 80$. The fuel utilization response is shown in Fig. 7(a). There is a big transient change after load changes, however the fuel utilization is eventually kept at the set point value by changing the fuel flow shown in Fig. 7(b). The maximum transient error of the fuel utilization is 3.76%, and the mean steady-state error is 0.13%.

The adaptive PID decoupling controller is used to adjust the temperature to their steady value (1200 K, 1113 K). The learning rate of the RBF neural network is $\beta = 0.08$, and the inertial coefficient of the RBF neural network is $\alpha = 0.03$. The proportion, integral and differential learning rate are $\eta_p = 0.08$, $\eta_i = 0.3$, $\eta_d = 0.4$. The PID parameters $k_p$, $k_i$ and $k_d$ are adjusted by self-learning RBF neural network until error approaching zero. The simulation results are shown in Fig. 8. There is a small temperature change after load changes, and the temperature is eventually kept the set point value. The maximum transient error of the SOFC operating temperature is 2.46%, and the mean steady-state error is 0.07%. The maximum transient error of the turbine inlet temperature is 2.52%, and the mean steady-state error is 0.08%.

## 5. Conclusions

The multi-loop control strategies for the SOFC/MGT hybrid system have been designed and discussed in the article. The mathematical model of the hybrid system is built firstly to generate the simulation data required for the dynamic RBF neural network identification model. Then the adaptive PID temperature decoupling controller and power model predictive controller are respectively developed to regulate the temperature and power. Moreover, the single neuron adaptive PID controller is employed to adjust the fuel utilization. Under the multi-loop control manner, the simulation results show that the temperature and fuel utilization can operate within the safety range, and at the same time the hybrid system can effectively track the desired power output fast and accurately with regard to load disturbances.

Besides, some other transient impacts besides the external load are not taken into consideration. Therefore, the extension of SOFC/MGT hybrid design and control implementation needs to be investigated in the future.

## Acknowledgment

This work is supported by National Natural Science Foundation of China (no. 50977007).

## References

[1] EG&G Technical Services, Inc., Fuel Cell Handbook, seventh edition. U.S. Department of Energy Office of Energy National Energy Technology Laboratory, Morgantown, West Virginia, November 2004.
[2] X.J. Wu, X.J. Zhu, G.Y. Cao, H.Y. Tu, Journal of Zhejiang University (Science A) 9 (5) (2008) 688–694.
[3] C. Stiller, B. Thorud, O. Bolland, R. Kandepu, L. Imsland, Journal of Power Sources 158 (1) (2006) 303–315.
[4] T. Kaneko, J. Brouwer, G.S. Samuelsen, Journal of Power Sources 160 (2006) 316–325.
[5] R. Kandepu, B.A. Foss, L. Imsland, Proceedings of the 2006 American Control Conference, Minneapolis, MN, USA, June 14–16, 2006.
[6] F. Mueller, R. Gaynor, A.E. Auld, et al., Journal of Power Sources 176 (2008) 229–239.
[7] J. Larminie, A. Dicks, Fuel Cell System Explained, Wiley, New York, 2004.
[8] X.J. Wu, Q. Huang, X.-j. Zhu, Journal of Power Sources 3 (1) (2011) 1295–1302.
[9] Q.M. Chen, PhD thesis, Shanghai Jiao Tong University, 2007.
[10] X.J. Wu, Q. Huang, X.J. Zhu, International Journal of Hydrogen Energy 36 (2011) 885–892.
[11] X.J. Wu, Q. Huang, X.J. Zhu, Journal of Fuel Cell Science And Technology, in press.
[12] S.H. Wang, J. Shen, Y.G. Li, Proceeding of the Chinese Society for Electrical Engineering 27 (26) (2007) 115–120.
[13] J.-K. Liu, Advanced PID Control MATLAB, second edition, Electronics Industry Press, Beijing, 2005.